Received: 16 June 2017 | Revised: 7 August 2017 | Accepted: 8 August 2017

DOI: 10.1002/aoc.4072

FULL PAPER

WILEY Applied Organometallic Chemistry

HAp-encapsulated γ-Fe_2O_3-supported dual acidic heterogeneous catalyst for highly efficient one-pot synthesis of benzoxanthenones and 3-pyranylindoles

Leila Kheirkhah | Manouchehr Mamaghani | Asieh Yahyazadeh | Nosrat Ollah Mahmoodi

Department of Chemistry, Faculty of Sciences, University of Guilan, PO Box 41335-1914, Rasht, Iran

Correspondence
Manouchehr Mamaghani, Department of Chemistry, Faculty of Sciences, University of Guilan, PO Box 41335-1914, Rasht, Iran.
Email: m-chem41@guilan.ac.ir; mchem41@gmail.com

A novel method is reported for the synthesis of benzoxanthenone and 3-pyranylindole derivatives via one-pot three-component reactions using a newly synthesized HAp-encapsulated γ-Fe_2O_3-supported dual acidic heterogeneous catalyst, as a reusable and highly efficient nanocatalyst. In this protocol the use of the nanocatalyst provided a green, useful and rapid method to generate products in short reaction times (4–20 min) and in excellent yields (87–96%). The paramagnetic nature of the catalyst provided a simple, trouble-free and facile approach for the separation of the catalyst by applying an external magnet, and it could be used in eight cycles without significant loss in catalytic efficiency.

KEYWORDS
benzoxanthenone, HAp-encapsulated, γ-Fe_2O_3, nanomagnetic catalyst, 3-pyranylindole, supported ionic liquid

1 | INTRODUCTION

Nanoparticles as heterogeneous catalysts have received significant attention as efficient catalysts in many organic reactions[1,2] due to their high surface-to-volume ratio, environmentally benign nature, reusability, simple work-up procedures and ease of isolation.[3,4] In particular, magnetic nanoparticles, have gained an effective role in organic synthesis[5] and the development of modern technology such as biomedicine and electronics[6–8] and have received increasing interest in recent years.[9–11] In addition, magnetic nanoparticles based on iron oxides are being used in clinical trials as contrast agents in magnetic resonance imaging, and clinical applications in drug delivery and diagnosis are seriously being considered.

Xanthene derivatives are important for having various biological and pharmaceutical activities such as antibacterial, antiviral, antimicrobial, antioxidant,[12] anti-inflammatory[13] and anticancer[14] activities. They can also be used as dyes, in laser technology and as pH-sensitive fluorescent materials for visualization of biomolecules.[15] Several procedures for the preparation of benzo[*a*]xanthene-11-one derivatives have been reported[16] using various catalysts such as $Zr(HSO_4)_4$,[17] $InCl_3$,[18] TCCA,[19] $NaHSO_4{\cdot}SiO_2$,[20] XSA,[21] $HClO_4{-}SiO_2$,[22] PWA,[23] nano-TiO_2,[24] Ph_3CCl,[25] $CeCl_3{\cdot}7H_2O$,[26] HY zeolite,[27] $Sr(OTf)_2$,[28] $RuCl_3{\cdot}nH_2O$ and ruthenium anchored on multi-walled carbon nanotubes.[29]

However, some of the reported methods suffer from one or more drawbacks such as use of expensive catalysts and strong Lewis acids, long reaction times, lower yields, use of toxic solvents and tedious catalyst separation and workup procedures.

Heterocycles containing pyran and indole structural moieties are another important class of compounds which possess broad scope of pharmaceutical and biological activities such as anti-inflammatory, anticonvulsant, cardiovascular and antibacterial activities, and also are present in various natural products such as alkaloids.[30–32] In particular, pyranylindoles with both structural units due

to their structural diversity and biological importance have become attractive targets for synthetic and medicinal chemists. However, there are only a limited number of reports of the synthesis and biological evaluation of these products.[33,34]

Therefore, there is scope for further innovation towards the development of new eco-friendly, economical and greener synthetic protocols that use highly efficient and reusable catalysts under mild reaction conditions in the synthesis of xanthene derivatives and pyranylindoles. In order to advance the development of environmentally friendly procedures and sustainable methods for the synthesis of these biologically important compounds, we report here a novel and practical protocol using a three-component one-pot reaction in the presence of a HAp-encapsulated γ-Fe_2O_3 [Fe_2O_3@HAp]-supported dual acidic nanocatalyst (**3**; Scheme 1) as a recyclable, heterogeneous and highly efficient catalyst.

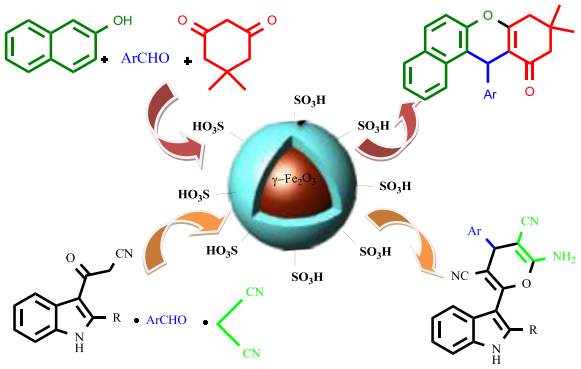

SCHEME 2 Synthesis of benzoxanthenones and 3-pyranylindoles in the presence of [Fe_2O_3@HAp]-supported dual acidic nanocatalyst **3**

2 | RESULTS AND DISCUSSION

A great interest has been sparked in the development of novel catalysts to facilitate various organic transformations under heterogeneous conditions. In addition, ionic liquids have also attracted much attention in recent years in synthetic organic chemistry as green catalysts. Thus, many efforts have been made by scientists to introduce new and novel catalysts which would combine the advantages of heterogeneous and ionic liquid catalysis.

In continuation of our research interests in the application of heterogeneous and ionic liquid catalysts for development of useful synthetic methodologies,[35–39] in the present article we report the synthesis and application of the novel [Fe_2O_3@HAp]-supported dual acidic nanocatalyst **3** (Scheme 1) in efficient, simple and facile one-pot three-component syntheses of benzo[*a*]xanthenone and 3-pyranylindole derivatives (Scheme 2).

Initially, *N*-(3-propyltriethoxysilane)imidazole (**1**) was prepared by the reaction of (3-chloropropyl) triethoxysilane and imidazole[40] which was then reacted with 1,4-butanesultone and further treated with sulfuric acid to give precursor ionic liquid (IL) **2**.[41] In the next step, [Fe_2O_3@HAp] nanocrystallites were prepared according to reported procedures.[3] Finally, a mixture of [Fe_2O_3@HAp] and IL **2** was heated in refluxing ethanol for 24 h to furnish the target supported dual acidic nanocatalyst **3** as a red powder in 95% yield (Scheme 1). The catalyst was characterized using various techniques such as Fourier transform infrared (FT-IR) spectroscopy, X-ray diffraction (XRD), energy-dispersive X-ray (EDX) analysis and thermogravimetric analysis (TGA) (Figure 1) and scanning electron microscopy (SEM) (Figure 2).

In the FT-IR spectrum (Figure 1a), the hydroxyl band appeared at 3422 cm^{-1}, the S=O group band appeared at 1384 cm^{-1} and the band of surface phosphate groups in the hydroxyapatite coating overlapped with S-O stretching peaks at 566 and 601 cm^{-1}. In XRD analysis (Figure 1b), the resulting pattern is in agreement with that of the syn structure of γ-Fe_2O_3 (1999JCPDS card no. 39–1346). Diffraction peaks at around 17.4°, 30.4°, 35.3°, 37.5°, 41.6°, 50.7°, 63.3°, 67.6° and 74.6° related to (110), (211), (220), (221), (311), (400), (422), (511) and (440) thoroughly confirm the presence of maghemite in the

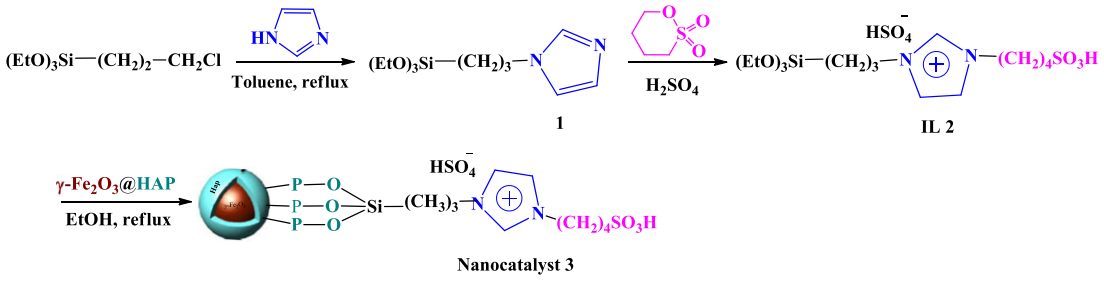

SCHEME 1 Synthesis of [Fe_2O_3@HAp]-supported dual acidic nanocatalyst **3**

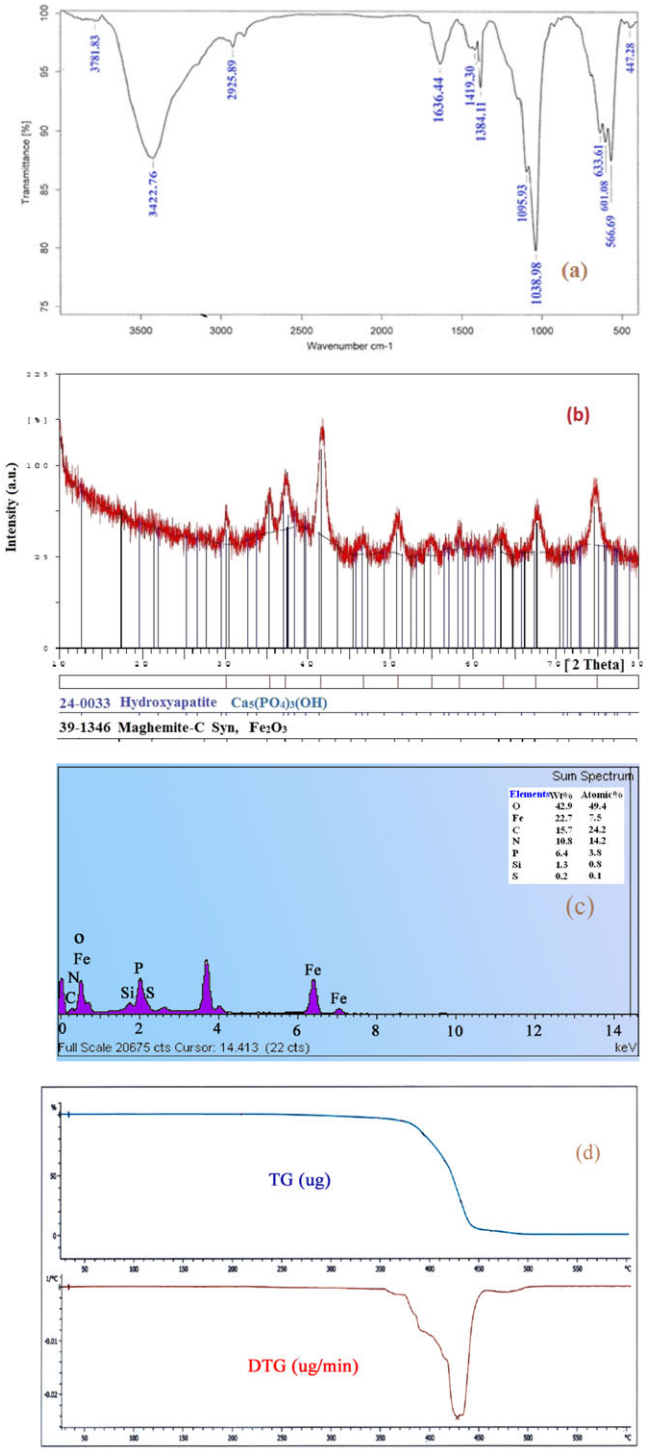

FIGURE 1 (a) FT-IR spectrum, (b) XRD pattern, (c) EDX analysis and (d) TGA curves

structure. In addition, characteristic diffraction peaks of HAp based on the standard XRD pattern of HAp (JCPDS card no. 24–0033) are readily recognized in the XRD pattern. The EDX spectrum of the nanocatalyst is presented in Figure 1(c). Signals of atoms such as Fe, Si, S, P and N related to the catalyst structure are seen in the spectrum. SEM analysis (Figure 2a) clearly shows that the particles of the catalyst are uniformly nanosized (40–50 nm). For comparison, SEM images of blank support (γ-Fe_2O_3@Hap; Figure 2b) and recycled catalyst (Figure 2c) after eight runs in the preparation of **5a** were obtained, which show that, after recycling, the morphology of the nanocatalyst has been retained. Thermal stability of the catalyst up to 380 °C is clearly confirmed from TGA and differential thermogravimetric (DTG) analysis (Figure 1d) and the weight loss in the temperature range 380–500 °C is mainly due to the thermal decomposition of the organic layer on the surface of the nanocatalyst.

After characterization of the catalyst, one-pot three-component reaction of 2-naphthol (**2**; 1 mmol), 4-nitrobenzaldehyde (**3b**; 1 mmol) and dimedone (**4**; 1 mmol) was used as a model system. The reaction mixture was heated in the presence of nanocatlyst **3** (0.02 g) in ethanol at 60 °C, which produced the product **5a** in 4 min and in 96% yield (Scheme 3). To optimize the reaction conditions, the preparation of **5a** was examined in several solvents, namely CH_3CN, 1,4-dioxane, CH_2Cl_2, water, ethylene glycol and ethanol, at various temperatures. The result showed that ethanol was the most effective solvent giving the product at 60 °C in excellent yield (Table 1, entry 3). The reaction at lower temperatures did not produce the desired products in reasonable yield (Table 1, entries 1 and 2). We also investigated the amount of catalyst in the preparation of **5a** and the best result was obtained using 0.02 g of nanocatalyst **3** per mmol of substrate at 60 °C in ethanol.

To compare the efficiency of nanaocatalyst **3** with that of various acidic and basic catalysts, the preparation of **5i** was carried out in ethanol (Table 2). It is evident from the results that the present catalyst is more efficient, in terms of product yield and reusability of the catalyst.

Using the optimized conditions, several benzo[*a*]xanthenone derivatives were synthesized (Scheme 3). The results are summarized in Table 3. It is clearly evident from the results that the reaction with both electron-withdrawing and electron-donating groups leads to products in short reaction times (4–16 min) and in excellent yields (87–96%).

We also examined the reusability of the catalyst. The nanocatalyst was separated from the reaction mixture simply using an external magnetic field (Figure 3), washed with hot ethanol, dried under vacuum and reused for subsequent reactions. After eight successive runs the activity of the catalyst, within the limits of experimental errors, remained almost unchanged (Figure 4).

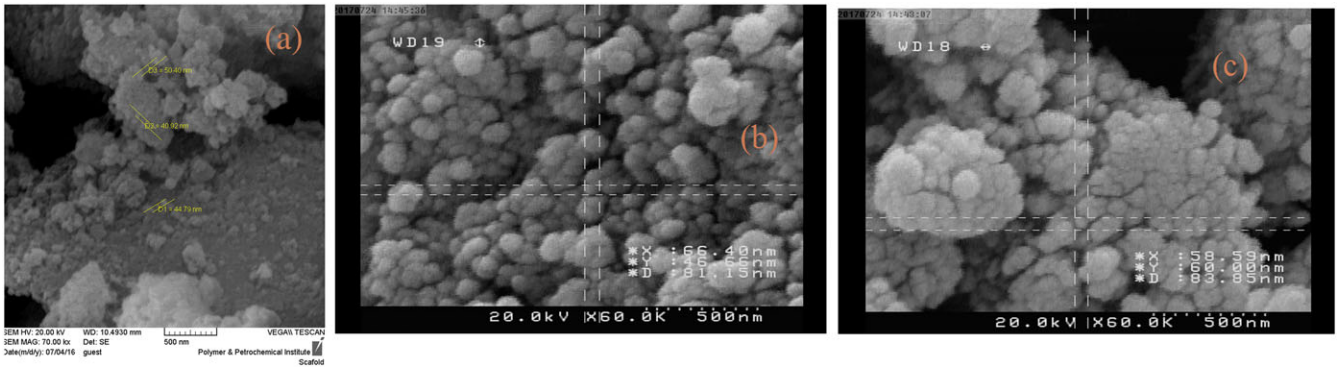

FIGURE 2 SEM images of (a) catalyst **3**, (b) blank support and (c) recycled catalyst after eight runs

A plausible mechanism of this multicomponent synthesis involves a Knoevenagel condensation/Michael addition cascade process. In the synthesis of benzo[*a*]xanthenones, the reaction proceeds through the *in situ* formation of *ortho*-quinonemethide intermediate by the nucleophilic addition of 2-naphthol derivative to aldehyde in the presence of nanocatalyst **3** which is further attacked by dimedone followed by cyclization and elimination of water to yield the desired target product **5** (Scheme 4).

Encouraged by these results, we extended the scope of this protocol to the synthesis of 3-pyranylindole derivatives (Scheme 5). Thus, the reaction of equimolar amounts of 3-cyanoacetylindole (**6**), arylaldehyde (**7**) and malononitrile (**8**) in the presence of catalyst **3** furnished the desired 3-pyranylindole derivatives in excellent yields (87–93%) and in short reaction times (6–20 min).

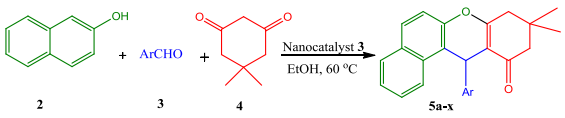

SCHEME 3 Synthesis of benzo[*a*]xanthenone derivatives using nanocatalyst **3**

To establish the optimum reaction conditions, the reaction between 3-cyanoacetyl-2-methylindole (1 mmol), 4-nitrobenzaldehyde (1 mmol) and malononitrile (1 mmol) was carried out in the presence of nanocatalyst **3** under various conditions. In order to choose suitable temperature and reaction media, various solvents such as dichloromethane, tetrahydrofuran (THF), 1,4-dioxane, ethanol and water as well as solvent-free conditions were used. The best results were obtained in ethanol at 60 °C using 0.02 g of nanocatalyst **3** per mmol of substrate producing the corresponding 3-pyranylindole (**9 h**) in 6 min and in 93% yield (Scheme 5; Table 4, entry 5). Various aryl aldehydes were reacted using the optimized conditions providing the desired 3-pyranylindoles in excellent yields (87–93%) and in short reaction times (6–20 min) (Table 5). The recyclability of the catalyst was also investigated using the preparation of **9 h** as a model reaction. The catalyst was separated using an external magnet as

TABLE 1 Effect of solvent on synthesis of benzo[*a*]xanthenone derivatives (**5a**) in the presence of nanaocatalyst **3**[a] at various temperatures

Entry	Solvent	Temperature (°C)	Time (min)	Yield (%)[b]
1	EtOH	25	120	45
2	EtOH	40	90	60
3	EtOH	60	4	96
4	EtOH	80	4	96
5	CH_3CN	60	120	Trace
6	1,4-Dioxane	100	180	Trace
7	CH_2Cl_2	40	60	55
8	H_2O	60	90	45
9	Ethylene glycol	120	120	40

[a]0.02 g of catalyst/mmol substrate.

[b]Isolated yield.

TABLE 2 Comparison of catalysts in the synthesis of **5i**

Entry	Ar	Catalyst[a]	Time (min)	Yield (%)[b]
1	3-BrC_6H_5	Nanocatalyst **3**	6	93 (this work)
2	3-BrC_6H_5	Il **2**	60	90 (this work)
3	3-BrC_6H_5	Fe_3O_4/CS-ag NPs	30	90[42]
4	3-BrC_6H_5	Orange peel	30	90[43]
5	3-BrC_6H_5	[pyridine–SO_3H]cl	9	90[44]
6	3-BrC_6H_5	*p*-TSA	120	91[45]
7	3-BrC_6H_5	Imidazole	60	Trace (this work)
8	3-BrC_6H_5	Product **1**	60	Trace (this work)

[a]Amount of catalyst used for entries: 1 (0.02 g), 2 (10%), 3 (0.015 g), 4 (0.05 g), 5 (3 mol%), 6 (10 mol%), 7 (10 mol%), 8 (10 mol%).

[b]Isolated yield.

TABLE 3 Synthesis of benzo[*a*]xanthenone derivatives (**5a–x**) under optimized conditions

Entry	Ar	Product	Time (min)	Yield (%)	M.p. (°C)
1	4-$O_2NC_6H_4$	**5a**	4	96	173–176 (175–178)[44]
2	2-ClC_6H_4	**5b**	8	90	177–179 (179–180)[46]
3	4-BrC_6H_4	**5c**	11	90	184–186 (185–187)[44]
4	4-$CH_3C_6H_4$	**5d**	16	87	174–176 (176–178)[46]
5	4-ClC_6H_4	**5e**	6	92	179–181 (180–182)[46]
6	C_6H_5	**5f**	11	93	149–151 (150–151)[46]
7	4-$CH_3OC_6H_4$	**5 g**	11	88	202–204 (204–205)[46]
8	3-$O_2NC_6H_4$	**5 h**	6	93	166–169 (168–170) [44]
9	3-BrC_6H_4	**5i**	6	93	160–163 (161–164)[44]
10	4-FC_6H_4	**5j**	7	94	183–185 (185–186) [46]
11	2,4-$Cl_2C_6H_3$	**5 k**	5	95	180–181 (181–182)[44]
12	5-CH_3thienyl	**5 l**	11	90	229–231
13	4-HOC_6H_4	**5 m**	6	91	222–224 (223–225)[46]
14	2-$CH_3OC_6H_4$	**5n**	16	92	166–167 (167–168)[46]
15	2-(2-nitrophenyl)acryl	**5o**	6	93	175–177
16	3-ClC_6H_4	**5p**	11	90	173–176 (175–178)[44]
17	3-OHC_6H_4	**5q**	11	90	238–241 (240–241)[44]
18	2-HOC_6H_4	**5r**	16	90	131–133 (135–137)[46]
19	2-$CH_3C_6H_4$	**5 s**	16	88	159–161 (160–163)[44]
20	3-$CH_3C_6H_4$	**5 t**	16	90	177–179 (178–180)[44]
21	2-BrC_6H_4	**5u**	11	91	169–171 (170–172)[44]
22	2-$O_2NC_6H_4$	**5w**	6	92	220–221 (220–222)[46]
23	2-Thienyl	**5x**	10	93	181–183 (183–184)[46]

in the previous protocol and used in the next run, which after eight consecutive runs did not show almost any decrease in the catalytic activity within the limits of experimental errors (Figure 5).

In the synthesis of 3-pyranylindoles the reaction proceeds through the *in situ* formation of intermediate **(i)** by the nucleophilic addition of 3-cyanoacetylindole to aldehyde in the presence of catalyst **3**. Intermediate **(i)**

FIGURE 3 Separation of catalyst from reaction mixture using an external magnet

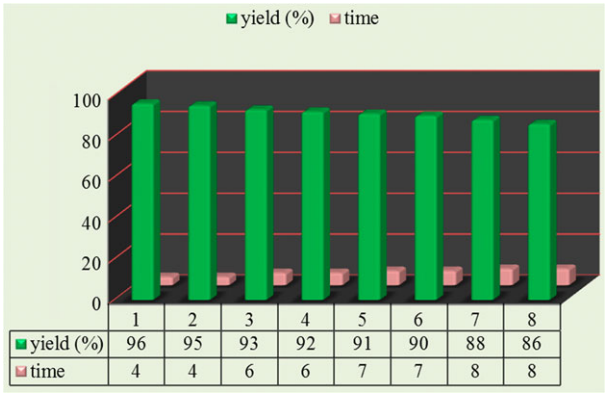

FIGURE 4 Reusability of catalyst **3** in synthesis of benzo[*a*]xanthenone **5a**

undergoes Michael addition with the tautomer of malononitrile to give **(ii)**. Compound **(ii)** enolizes to afford intermediate **(iii)** which gives **(iv)** by nucleophilic addition of hydroxyl group to the cyano group. Finally **(iv)** rearranges via hydrogen transfer to yield 3-pyranylindole derivatives **9a–k** (Scheme 6).

The reaction profile of the present protocol is very clean and no side-products are formed.

The structures of all the newly synthesized products were confirmed using spectroscopic (IR, ^{1}H NMR, ^{13}C NMR) and elemental analyses. For the known derivatives, their spectroscopic data and melting points were compared with those of literature reports.

3 | CONCLUSIONS

In summary, we have reported the synthesis of tetrahydrobenzo[*a*]xanthene-11-ones and 3-pyranylindole derivatives using [Fe_2O_3@HAp]-supported dual acidic nanocatalyst as a new, heterogeneous and reusable catalyst in green media. This protocol involves mild reaction conditions, excellent yields and short reaction times. A green and cost-effective catalyst, an easy work-up procedure and avoiding the use of large volumes of hazardous organic solvents make it a useful alternative to previously applied procedures. Also, the magnetic nature of the nanoparticles allows for easy recovery using an external magnetic field and subsequent recycling of the catalyst.

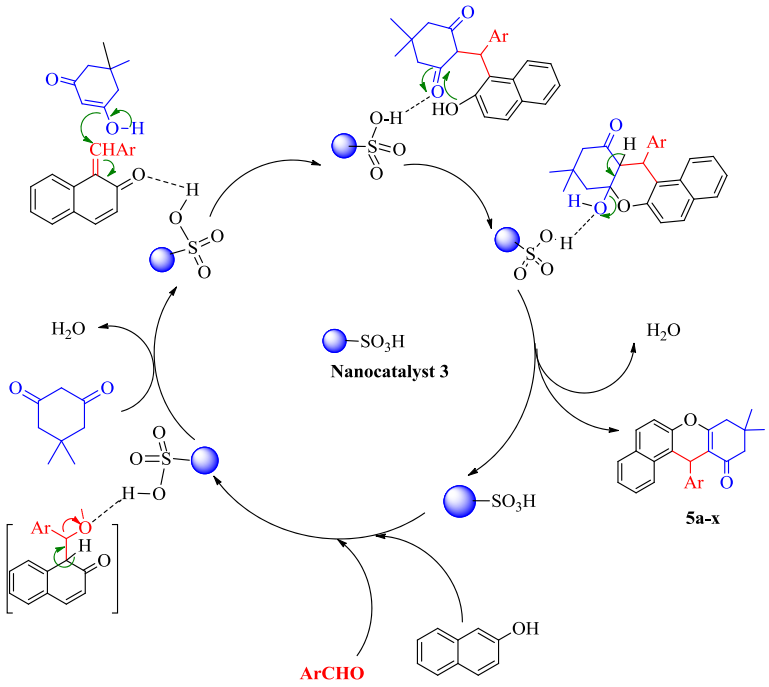

SCHEME 4 Plausible reaction mechanism for synthesis of benzo[*a*]xanthenone derivatives using nanocatalyst **3**

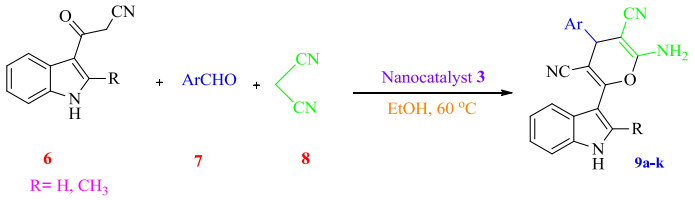

SCHEME 5 Synthesis of 3-pyranylindole derivatives using nanocatalyst **3**

TABLE 4 Effect of solvent on synthesis of 3-pyranylindole derivatives (**9 h**) in the presence of nanaocatalyst **3**[a] at various temperatures

Entry	Solvent	Temperature (°C)	Time (min)	Yield (%)[b]
1	THF	65	120	45
2	1,4-Dioxane	100	120	93
3	EtOH	25	30	50
4	EtOH	45	30	61
5	EtOH	60	6	93
6	EtOH	80	6	91
7	CH_2Cl_2	40	60	35
8	H_2O	100	90	25
9	Solvent-free	60	85	70

[a]0.02 g of catalyst/mmol substrate.

[b]Isolated yield.

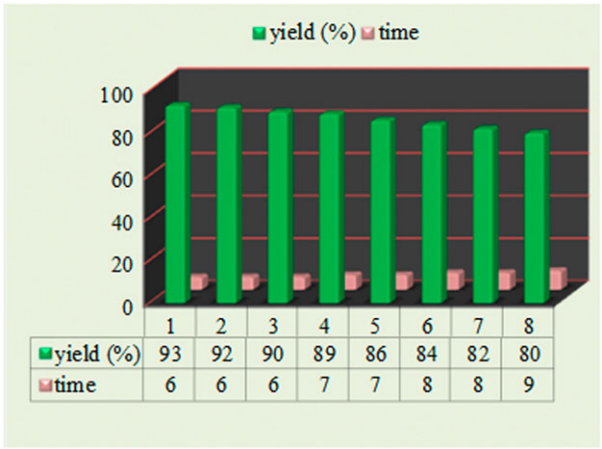

FIGURE 5 Reusability of nanocatalyst **3** in synthesis of 3-pyranylindole **9 h**

4 | EXPERIMENTAL

4.1 | General

Melting points were measured with an Electrothermal 9100 apparatus. IR spectra were obtained with on a Shimadzo IR-470 spectrometer. ^{1}H NMR and ^{13}C NMR spectra were recorded with a 400 MHz Bruker DRX-400 in DMSO-d_6 using tetramethylsilane as an internal standard. Elemental analyses were performed with a Carlo-Erba EA1110CNNO-S analyser and agreed (within 0.30) with the calculated values. XRD was carried out with a Philips X-Pert MPD diffractometer using a Co tube. SEM images were obtained with a Philips XL30 electron microscope. All chemicals were purchased from Merck and

TABLE 5 Synthesis of 3-pyranylindole derivatives (**9a–k**)

Entry	Ar	R	Product	Time (min)	Yield (%)[a]	M.p. (°C)	
1	4-ClC_6H_4	H	**9a**	11	90	258–261	260–262[34]
2	2-ClC_6H_4	H	**9b**	16	88	211–213	214–216[34]
3	C_6H_5	H	**9c**	18	91	221–223	224–226[34]
4	4-FC_6H_4	H	**9d**	10	89	253–256	256–258[34]
5	3-$O_2NC_6H_4$	H	**9e**	10	93	241–243	242–244[34]
6	2-Thienyl	H	**9f**	20	87	224–227	226–228[34]
7	3-BrC_6H_4	CH_3	**9 g**	13	90	239–241	(this work)
8	4-$O_2NC_6H_4$	CH_3	**9 h**	6	93	290–291	(this work)
9	3-HOC_6H_4	CH_3	**9i**	17	88	217–219	(this work)
10	4-BrC_6H_4	CH_3	**9j**	12	90	256–258	(this work)
11	3-$O_2NC_6H_4$	CH_3	**9 k**	11	91	261–263	(this work)

[a]Isolated yield.

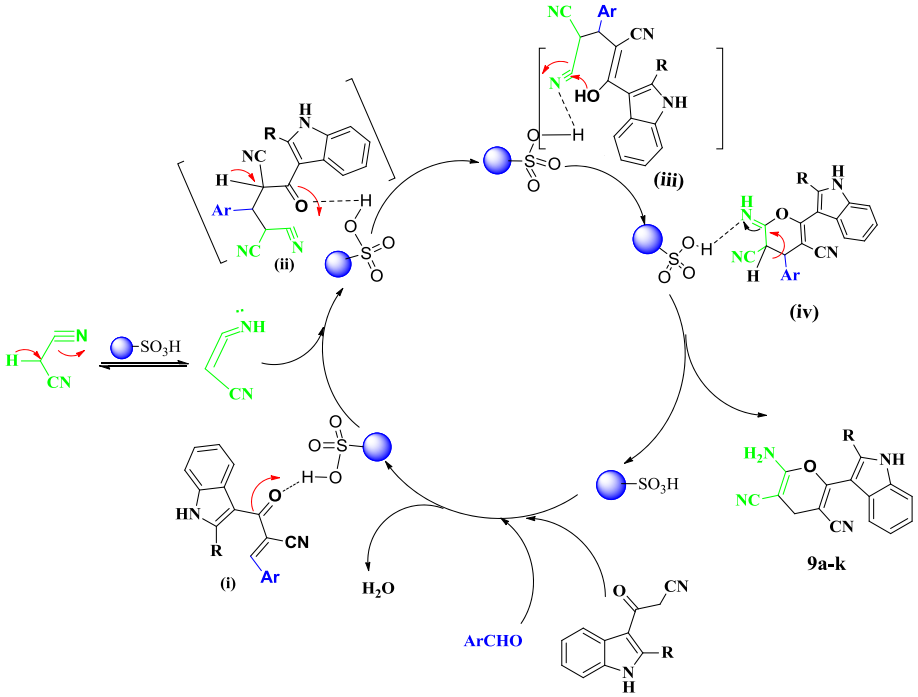

SCHEME 6 Plausible reaction mechanism for synthesis of 3-pyranylindole derivatives using catalyst **3**

used without further purification. All solvents used were dried and distilled according to standard procedures.

4.2 | Grafting of 3-sulfobutyl-1-(3-propyltriethoxysilane)imidazolium hydrogen sulfate on [Fe_2O_3@HAp] (3)

N-(3-Propyltriethoxysilane)imidazole (**1**), 3-sulfobutyl-1-(3-propyltriethoxysilane)imidazolium hydrogen sulfate (IL **2**) and [Fe_2O_3@HAp] were synthesized according to procedures reported in the literature.[34,35] To a solution of IL **2** (1.0 g) in absolute ethanol (30 ml), [Fe_2O_3@HAp] (2.0 g) was added. The mixture was refluxed overnight under an argon atmosphere. The solvent was removed using a rotatory evaporator. The resulting magnetic nanoparticles were separated using an external magnet device (Figure 2) and washed twice with diethyl ether (100 ml) then dried under vacuum at room temperature to afford the supported dual acidic nanocatalyst **3** as a red powder in 95% yield.

4.3 | General procedure for synthesis of 12-aryl-8,9,10,12-tetrahydrobenzo[*a*]-xanthen-11-one derivatives

To a mixture of aldehyde (1 mmol), 2-naphthol (1 mmol) and dimedone (1 mmol) was added dual acidic nanaocatalyst **3** (0.02 g) and the reaction mixture was stirred mechanically in ethanol (1 ml) at 60 °C. After completion of the reaction, which was monitored by TLC, the reaction mixture was diluted with hot ethanol and the catalyst was easily separated from the reaction mixture using an external magnet. The catalyst was washed with ethanol and dried for reuse in the next run. The combined organic solution was concentrated and the solid product obtained was collected by filtration and washed with ethanol to afford the desired pure product (**5a–x**).

4.4 | Selected spectral data of 12-aryl-8,9,10,12-tetrahydrobenzo[*a*]-xanthen-11-one derivatives (Table 3)

9,10-Dihydro-9,9-dimethyl-12-((5-methylthiophen-2-yl) methyl)-8*H*–benzo[*α*]xanthen-11(12*H*)-one (**5 l**). Creamy solid; m.p. 229–231 °C. IR (KBr, ν, cm^{-1}): 2959, 1651 (CO), 1222, 1173. ^{1}H NMR (400 MHz, $CDCl_3$, δ, ppm): 8.11 (d, 1H, J = 8.4 Hz, Ar-H), 7.96 (d, 1H, J = 7.2 Hz, Ar-H), 7.95 (d, 1H, J = 9.2 Hz, Ar-H), 7.58 (dt, 1H, J = 6.8, 1.4 Hz, Ar-H), 7.50 (dt, 1H, J = 8.0, 1.2 Hz, Ar-H),7.44 (d, 1H, J = 9.2 Hz Ar-H), 6.62 (d, 1H, J = 3.6 Hz, Ar-H), 6.46 (m, 1H, Ar-H), 5.84 (s, 1H), 2.70, 2.68 (d, 2H, J = 17.4 Hz, CH_2), 2.39, 2.24 (d, 2H, J = 15.8 Hz, CH_2), 2.24 (s, 3H), 1.1 (s, 3H, CH_3), 1.02 (s, 3H, CH_3). ^{13}C NMR (100 MHz, $CDCl_3$, δ, ppm): 196.4, 164.8, 147.5, 146.5, 138.2, 131.5, 131.1, 129.7, 129.1, 127.8, 125.6, 125.1, 124.9, 123.6, 117.6, 117.3, 113.2, 50.6, 40.6, 32.4, 31.2, 29.3, 26.9, 15.3. Anal.

Calcd for $C_{24}H_{22}O_2S$ (374.5) (%): C, 76.97; H, 5.92. Found (%): C, 76.81; H, 5.74.

9,9-Dimethyl-12-(1-(2-nitrophenyl)vinyl)-9,10-dihydro-8*H*-benzo[*a*]xanthen-11(12*H*)-one (**5o**). Creamy solid; m.p. 175–177 °C. IR (KBr, ν, cm^{-1}): 2941, 1649 (CO), 1515, 1376, 1226. ^1H NMR (400 MHz, $CDCl_3$, δ, ppm): 8.14 (d, 1H, J = 8.4 Hz, Ar-H), 7.96 (t, 2H, J = 9.4 Hz, Ar-H), 7.86 (d, 1H, J = 8.0 Hz, Ar-H), 7.63 (t, 1H, J = 7.4 Hz, Ar-H), 7.58 (m, 2H, Ar-H), 7.52 (t, 1H, J = 7.2 Hz, Ar-H), 7.45–7.41 (m, 2H, Ar-H), 6.55 (s, 1H, CH_2=), 6.54 (s, 1H, CH_2=) 5.25 (s, 1H), 2.7, 2.6 (d, 2H, J = 17.4 Hz, CH_2), 2.4, 2.3 (d, 2H, J = 16.0 Hz, CH_2), 1.12 (s, 6H, CH_3). ^{13}C NMR (100 MHz, $CDCl_3$, δ, ppm): 196.6, 165.5, 147.9, 147.8, 137.0, 133.8, 131.6, 131.4, 131.3, 129.7, 129.0, 128.9, 128.5, 127.8, 125.6, 125.4, 124.6, 123.9, 117.6, 115.9, 111.1, 50.7, 40.8, 32.4, 31.6, 29.3, 27.2. Anal. Calcd for $C_{27}H_{23}NO_4$ (425.48) (%): C, 76.22; H, 5.45; N, 3.29. Found (%): C, 76.11; H, 5.24; N, 3.17.

4.5 | General procedure for synthesis of 3-pyranylindole derivatives

To a mixture of 3-cyanoacetylindole or 2-methyl-3-cyanoacetylindole (1 mmol), arylaldehyde (1 mmol) and malononitrile (1 mmol) was added dual acidic nanocatalyst **3** (0.02 g) and the reaction mixture was stirred mechanically in ethanol (1 ml) at 60 °C. After completion of the reaction, which was monitored by TLC, the reaction mixture was diluted with hot ethanol and the catalyst was easily separated from the reaction mixture using an external magnet. The catalyst was washed with ethanol and dried for reuse in the next run. The combined organic solution was concentrated and the solid product obtained was collected by filtration and washed with ethanol to furnish the desired pure product (**9a**–**k**).

4.6 | Selected spectral data of 3-pyranylindole derivatives (Table 5)

2-Amino-4-(3-bromophenyl)-6-(2-methyl-1*H*-indol-3-yl)-4*H*–pyran-3,5-dicarbonitrile (**9 g**). White solid; m.p. 239–241 °C. IR (KBr, ν, cm^{-1}): 3472, 3321 (N—H stretch), 2192 (CN stretch). ^1H NMR (400 MHz, $CDCl_3$, δ, ppm): 11.82 (br. s, 1H, NH), 7.60 (d, 1H, J = 1.2 Hz, Ar-H), 7.59–7.57 (m, 1H, Ar-H), 7.49–7.44 (m, 3H, Ar-H), 7.39 (d, 1H, J = 7.6 Hz, Ar-H), 7.32 (br. s, 2H, NH_2), 7.17 (t, 1H, J = 7.0 Hz, Ar-H), 7.12 (t, 1H, J = 7.2 Hz, Ar-H), 4.58 (s, 1H, C—H), 2.44 (s, 3H, CH_3). ^{13}C NMR (100 MHz, $CDCl_3$, δ, ppm): 159.5, 156.4, 146.3, 139.7, 135.4, 131.8, 131.2, 130.8, 127.3, 126.3, 122.6, 122.3, 120.8, 119.7, 119.6, 118.1, 111.8, 103.5, 90.0, 55.6, 39.3, 13.9. Anal. Calcd for $C_{22}H_{15}BrN_4O$ (431.28) (%): C, 61.27; H, 3.51; N, 12.99. Found (%): C, 61.10; H, 3.38; N, 12.82.

2-Amino-6-(2-methyl-1*H*-indol-3-yl)-4-(4-nitrophenyl)-4*H*–pyran-3,5-dicarbonitrile (**9 h**). Yellow solid; m.p. 290–291 °C. IR (KBr, ν, cm^{-1}): 3486, 3303 (N—H stretch), 2200 (CN stretch). ^1H NMR (400 MHz, $CDCl_3$, δ, ppm): 11.84 (br. s, 1H, NH), 8.34 (d, 2H, J = 8.6 Hz, Ar-H), 7.72 (d, 2H, J = 8.6 Hz, Ar-H), 7.49 (d, 1H, J = 8.0 Hz, Ar-H), 7.42–7.39 (m, 3H, NH_2, Ar-H), 7.17 (td, 1H, J = 7.4, 1.0 Hz, Ar-H), 7.12 (td, 1H, J = 7.2, 1.0 Hz, Ar-H), 4.78 (s, 1H, C—H), 2.44 (s, 3H, CH_3). ^{13}C NMR (100 MHz, $CDCl_3$, δ, ppm): 159.6, 156.7, 150.9, 147.6, 139.9, 135.4, 129.6, 126.3, 124.8, 122.3, 120.8, 119.7, 119.5, 118.0, 111.8, 103.4, 89.3, 55.1, 39.3, 14.0. Anal. Calcd for $C_{22}H_{15}N_5O_3$ (397.39) (%): C, 66.49; H, 3.80; N, 17.62. Found (%): C, 66.35; H, 3.60; N, 17.43.

2-Amino-4-(3-hydroxyphenyl)-6-(2-methyl-1*H*-indol-3-yl)-4*H*–pyran-3,5-dicarbonitrile (**9i**). White solid; m.p. 217–219 °C. IR (KBr, ν, cm^{-1}): 3449, 3336 (N—H stretch), 2211 (CN stretch). ^1H NMR (400 MHz, $CDCl_3$, δ, ppm): 11.78 (br. s, 1H, NH), 9.58 (br. s, 1H, OH), 7.46 (d, 1H, J = 7.6 Hz, Ar-H), 7.39 (d, 1H, J = 8.0 Hz, Ar-H), 7.24 (t, 1H, J = 7.6 Hz, Ar-H), 7.21 (br.s, 2H, NH_2), 7.16 (td, 1H, J = 7.2, 1.2 Hz, Ar-H), 7.11 (td, 1H, J = 7.4, 1.2 Hz, Ar-H), 6.81–6.73 (m, 3H, Ar-H), 4.36 (s, 1H, C—H), 2.43 (s, 3H, CH_3). ^{13}C NMR (100 MHz, $CDCl_3$, δ, ppm): 159.4, 158.3, 155.9, 145.1, 139.4, 135.4, 130.4, 126.4, 122.3, 120.7, 119.8, 119.6, 118.6, 118.3, 115.3, 114.6, 111.7, 103.6, 90.9, 56.3, 39.3, 13.85. Anal. Calcd for $C_{22}H_{16}N_4O_2$ (368.39) (%): C, 71.73; H, 4.38; N, 15.21. Found (%): C, 71.58; H, 4.25; N, 15.33.

2-Amino-4-(4-bromophenyl)-6-(2-methyl-1*H*-indol-3-yl)-4*H*–pyran-3,5-dicarbonitrile (**9j**). White solid; m.p. 256–258 °C. IR (KBr, ν, cm^{-1}): 3482, 3328 (N—H stretch), 2197 (CN stretch). ^1H NMR (400 MHz, $CDCl_3$, δ, ppm): 11.80 (br. s, 1H, NH), 7.67 (d, 2H, J = 8.4 Hz, Ar-H), 7.47 (d, 1H, J = 7.6 Hz, Ar-H), 7.39 (d, 1H, J = 7.6 Hz, Ar-H), 7.38 (d, 2H, J = 8.4 Hz, Ar-H), 7.30 (br. s, 2H, NH_2), 7.16 (td, 1H, J = 7.5, 1.2 Hz, Ar-H), 7.11 (td, 1H, J = 7.5, 1.2 Hz, Ar-H), 4.55 (s, 1H, C—H), 2.43 (s, 3H, CH_3). ^{13}C NMR (100 MHz, $CDCl_3$, δ, ppm): 159.5, 156.2, 143.1, 139.6, 135.5, 132.4, 130.4, 126.4, 122.3, 121.5, 120.8, 119.74, 119.70, 118.2, 111.8, 103.6, 90.2, 55.7, 39.3, 14.0. Anal. Calcd for $C_{22}H_{15}BrN_4O$ (431.28) (%): C, 61.27; H, 3.51; N, 12.99. Found (%): C, 61.15; H, 3.32; N, 12.87.

2-Amino-6-(2-methyl-1*H*-indol-3-yl)-4-(3-nitrophenyl)-4*H*–pyran-3,5-dicarbonitrile (**9 k**). Yellow solid; m.p. 261–263 °C. IR (KBr, ν, cm^{-1}): 3406, 3305 (N—H stretch), 2199 (CN stretch). ^1H NMR (400 MHz, $CDCl_3$, δ, ppm): 11.84 (br. s, 1H, NH), 8.27–8.24 (m, 2H, Ar-H), 7.94 (d, 1H, J = 8.0 Hz, Ar-H), 7.80 (t, 1H, J = 7.8 Hz, Ar-H),

7.50 (d, 1H, J = 7.6 Hz, Ar-H), 7.41(br. s, 2H, NH_2), 7.40 (d, 1H, J = 7.6 Hz, Ar-H), 7.17 (td, 1H, J = 7.5, 1.4 Hz, Ar-H), 7.12 (td, 1H, J = 7.5, 1.0 Hz, Ar-H), 4.84 (s, 1H, C—H), 2.46 (s, 3H, CH_3). ^{13}C NMR (100 MHz, $CDCl_3$, δ, ppm): 159.7, 156.8, 148.6, 145.8, 139.9, 135.5, 135.0, 131.3, 126.4, 123.4, 122.6, 122.4, 120.8, 119.7, 119.6, 118.1, 111.8, 103.5, 89.5, 55.3, 39.3, 14.0. Anal. Calcd for $C_{22}H_{15}N_5O_3$ (397.39) (%): C, 66.49; H, 3.80; N, 17.62. Found (%): C, 66.31; H, 3.65; N, 17.55.

ACKNOWLEDGEMENT

The authors are grateful to the Research Council of University of Guilan for financial support of this research work.

ORCID

Manouchehr Mamaghani http://orcid.org/0000-0002-2054-8685

REFERENCES

[1] X. Collard, L. Li, W. Lueangchaichaweng, A. Bertrand, C. Aprile, P. P. Pescarmona, *Catal. Today* **2014**, *235*, 184.

[2] M. A. Ghasemzadeh, J. Safaei-Ghomi, S. Zahedi, *J. Serb. Chem. Soc.* **2013**, *78*, 769.

[3] L. Ma'mani, M. Sheykhan, A. Heydari, M. Faraji, Y. Yamini, *Appl. Catal.* **2010**, *377*, 64.

[4] J. Deng, L. P. Mo, F. Y. Zhao, *Green Chem.* **2011**, *13*, 2576.

[5] M. A. Ghasemzadeh, *Acta Chim. Slov.* **2015**, *62*, 977.

[6] A. Hutten, D. Sudfeld, I. Ennen, G. Reiss, W. Hachmann, U. Heinzmann, K. Wojczykowski, P. Jutzi, W. Saikaly, G. Thomas, *J. Biotechnol.* **2004**, *112*, 47.

[7] P. Tartaj, M. P. Morales, S. Veintemillas-Verdaguer, T. Gonzalez-Carreno, C. J. Serna, *J. Phys. D* **2003**, *36*, 182.

[8] D. Ho, X. Sun, S. Sun, *Acc. Chem. Res.* **2011**, *44*, 875.

[9] C. J. Serpell, J. Cookson, D. Ozkaya, P. D. Beer, *Nat. Chem.* **2011**, *3*, 478.

[10] M. Christine, D. Astruc, *Chem. Rev.* **2004**, *104*, 293.

[11] A. H. Lu, E. L. Salabas, F. Schueth, *Angew. Chem. Int. Ed* **2007**, *46*, 1222.

[12] R. Tayebee, S. Tizabi, *Chinese J. Catal.* **2012**, *33*, 962.

[13] J. M. Khurana, A. Chaudhary, A. Lumb, B. Nand, *Can. J. Chem.* **2012**, *90*, 739.

[14] A. C. Navarro, C. Sierra, C. Ochoa-Puentes, *RSC Adv.* **2016**, *6*, 65355.

[15] A. A. Mehmandoost, N. Salehi, M. Ghashang, *World Appl. Sci. J.* **2011**, *15*, 261.

[16] D. Biswanath, B. Ravikanth, R. Ramu, K. Laxminarayana, B. Vittal Rao, *J. Mol. Catal A* **2006**, *255*, 74.

[17] N. Foroughifar, A. Mobinikhaledi, H. Moghanian, *Int. J. Green Nanotechnol. Phys. Chem.* **2009**, *1*, 57.

[18] H. R. Tavakoli, H. Zamani, M. H. Ghorbani, H. Etedali Habibabadi, *Iran J. Chem.* **2009**, *2*, 118.

[19] B. Maleki, M. Gholizadeh, Z. Sepehr, *Bull. Korean Chem. Soc.* **2011**, *32*, 1697.

[20] B. Das, K. Laxminarayana, M. Krishnaiah, Y. Srinivas, *Synlett* **2007**, *20*, 3107.

[21] H. Rajesh, D. Vekariya, *ARKIVOC* **2015**, *1*, 70.

[22] B. Das, D. Nandan Kumar, K. Laxminarayana, B. Ravikanth, *Helv. Chim. Acta* **2007**, *90*, 1330.

[23] H. J. Wang, X. Q. Ren, Y. Y. Zhang, Z. H. Zhang, *J. Braz. Chem. Soc.* **2009**, *28*, 1939.

[24] A. Khazaei, A. R. Moosavi-Zare, Z. Mohammadi, A. Zare, V. Khakyzadeh, G. Darvishi, *RSC Adv.* **2013**, *3*, 1323.

[25] A. Zare, M. Merajoddina, M. A. Zolfigol, *Iran. J. Catal.* **2013**, *3*, 83.

[26] M. Kidwai, A. Jahan, N. K. Mishra, *C. R. Chim.* **2012**, *15*, 324.

[27] V. Rama, K. Kanagaraj, K. Pitchumani, *Tetrahedron Lett.* **2012**, *53*, 1018.

[28] J. Li, W. Tang, L. Lu, W. Su, *Tetrahedron Lett.* **2008**, *49*, 7117.

[29] a) K. Tabatabaeian, M. A. Zanjanchi, M. Mamaghani, A. Dadashi, *Res. Chem. Intermed.* **2016**, *42*, 5049. b) K. Tabatabaeian, A. Khorshidi, M. Mamaghani, A. Dadashi, M. Khoshnood Jalali, *Can. J. Chem.* **2011**, *89*, 623.

[30] L. Bonsignore, G. Loy, D. Secei, A. Calignano, *Eur. J. Med. Chem.* **1993**, *28*, 517.

[31] F. M. Abderlrazek, P. Metz, O. Kataeva, A. Jager, S. F. El-Mahrouky, *Arch. Pharm.* **2007**, *340*, 543.

[32] M. E. Huwaida Hassaneen, M. R. Pagni, *Z. Naturforsch* **2010**, *65b*, 1491.

[33] V. Kalalawe, R. Kagne, D. Munde, *Int. J. Innov. Sci. Eng. Technol.* **2016**, *3*, 2348.

[34] a) N. Lakshmi, P. Thirumurugan, K. M. Noorulla, P. T. Perumal, *Bioorg. Med. Chem. Lett.* **2010**, *20*, 5054. b) P. Borah, P. S. Naidu, S. Majumder, P. J. Bhuyan, *Mol. Diversity* **2014**, *18*, 759.

[35] M. Mamaghani, F. Shirini, M. Sheykhan, M. Mohsenimehr, *RSC Adv.* **2015**, *5*, 44524.

[36] M. Seddighi, F. Shirini, M. Mamaghani, *C. R. Chim.* **2015**, *18*, 573.

[37] M. Mamaghani, F. Shirini, N. O. Mahmoodi, A. Azimi-Roshan, H. Hashemlou, *J. Mol. Struct.* **2013**, *1051*, 169.

[38] L. Kheirkhah, M. Mamaghani, N. O. Mahmoodi, A. Yahyazadeh, A. Fallah Shojaei, Y. Rostamli, *J. Chin. Chem. Soc.* **2016**, *63*, 410.

[39] M. Mamaghani, F. Shirini, E. Bassereh, R. Hossein Nia, J. Saudi, *Chem. Soc.* **2016**, *20*, 570.

[40] A. M. Lazarin, Y. Gushikem, S. C. de Castro, *J. Mater. Chem.* **2000**, *10*, 2526.

[41] Q. Zhang, J. Luo, Y. Wei, *Green Chem.* **2010**, *12*, 2246.

[42] R. Mohammadi, E. Eidi, M. Ghavami, M. Z. Kassaee, *J. Mol. Catal. A* **2014**, *393*, 309.

[43] F. Taghavi, M. Gholizadeh, A. S. Saljooghi, M. Ramezani, *RSC Adv.* **2016**, *6*, 87082.

[44] A. R. Moosavi-Zare, M. A. Zolfigol, M. Zarei, A. Zare, V. Khakyzadeh, *J. Mol. Liq.* **2013**, *186*, 63.

[45] J. M. Khurana, D. Magoo, *Tetrahedron Lett.* **2009**, *50*, 4777.

[46] B. Sadeghi, *Sci. Iranica* **2014**, *21*, 708.

SUPPORTING INFORMATION

Additional Supporting Information may be found online in the supporting information tab for this article.

How to cite this article: Kheirkhah L, Mamaghani M, Yahyazadeh A, Mahmoodi NO. HAp-encapsulated γ-Fe_2O_3-supported dual acidic heterogeneous catalyst for highly efficient one-pot synthesis of benzoxanthenones and 3-pyranylindoles. *Appl Organometal Chem*. 2017; e4072. https://doi.org/10.1002/aoc.4072